CO_2 Hydrogenation to Methanol on Tungsten-Doped Cu/CeO_2 Catalysts

Yong Yan, Roong Jien Wong, Zhirui Ma, Felix Donat, Shibo Xi, Syed Saqline, Qianwenhao Fan, Yonghua Du, Armando Borgna, Qian He, Christoph R. Müller, Wei Chen, Alexei A. Lapkin, Wen Liu[1]

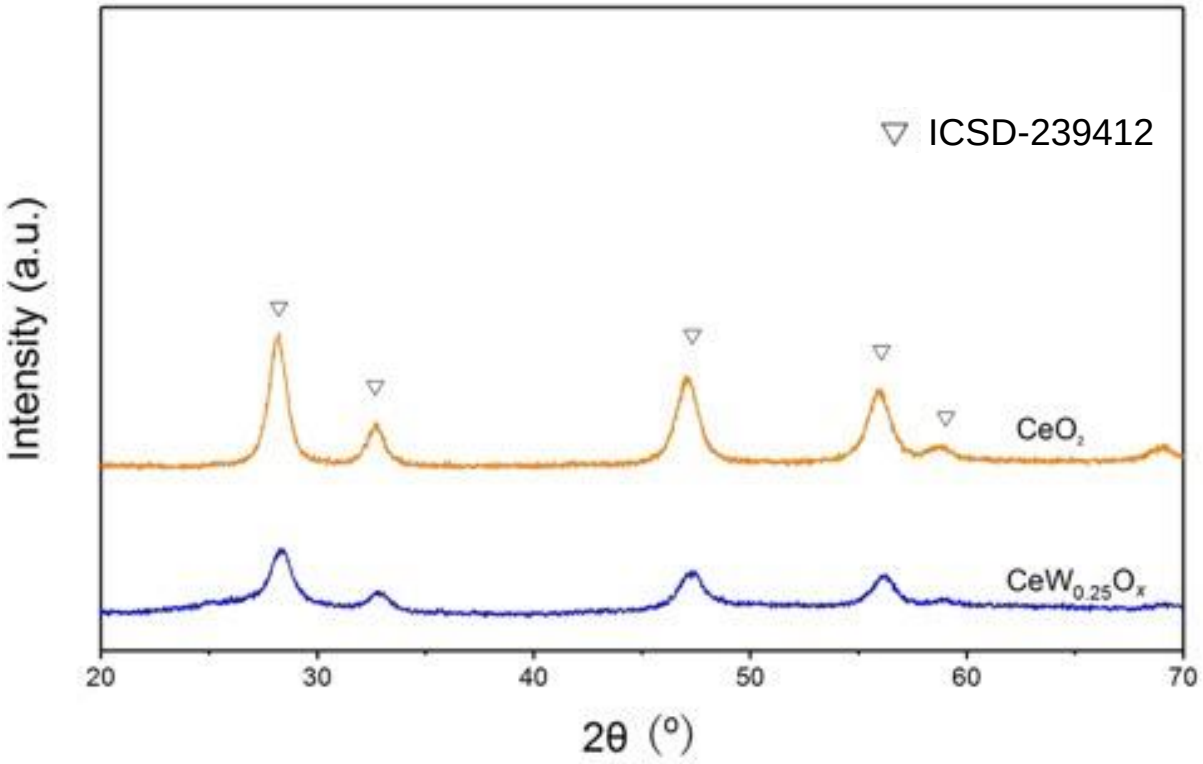

Figure S1. XRD patterns of as-calcined supports.

[1] Corresponding author: wenliu@ntu.edu.sg

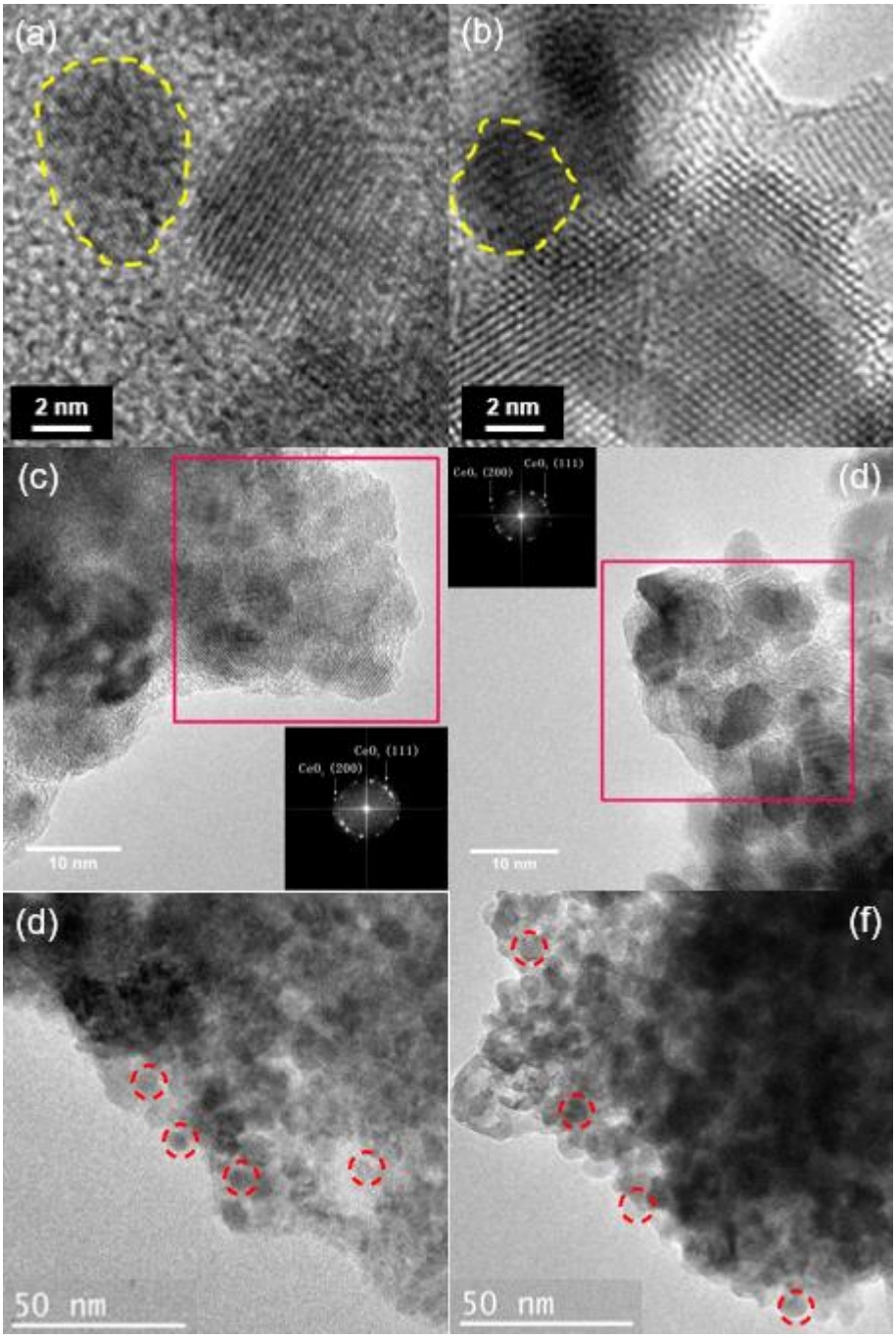

Figure S2. HRTEM images of (a, c, e) Cu/CeO_2 and (b, d, f) $Cu/CeW_{0.25}O_x$ catalysts. The yellow outlines in (a) and (b) highlight grains of Cu. The insets in (c) and (d) show SAED of the selected areas in red. The red circles in (d) and (f) highlight Cu particles.

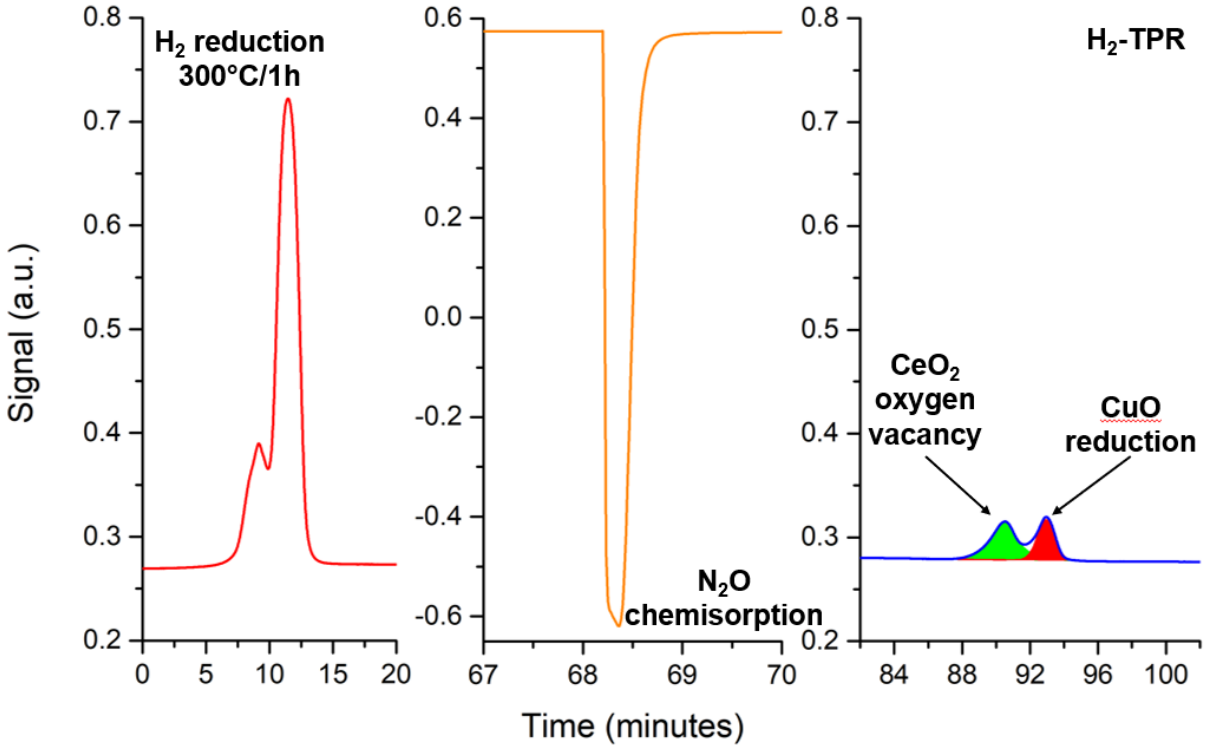

Figure S3. N_2O chemisorption profile of Cu/CeO_2 during (left) pre-reduction, (middle) N_2O chemisorption and (right) H_2-TPR. The first peak during H_2-TPR is assigned to the creation of oxygen vacancies on the CeO_2 support vacancy due to hydrogen spillover across the Cu/CeO_2 interface. Therefore, only the second TPR peak, which corresponds to the removal of surface oxygen monolayer from Cu particles, is used for estimating the Cu dispersion. CeO_2 oxygen vacancy peak was not observed in $Cu/CeW_{0.25}O_x$ during the H_2-TPR stage.

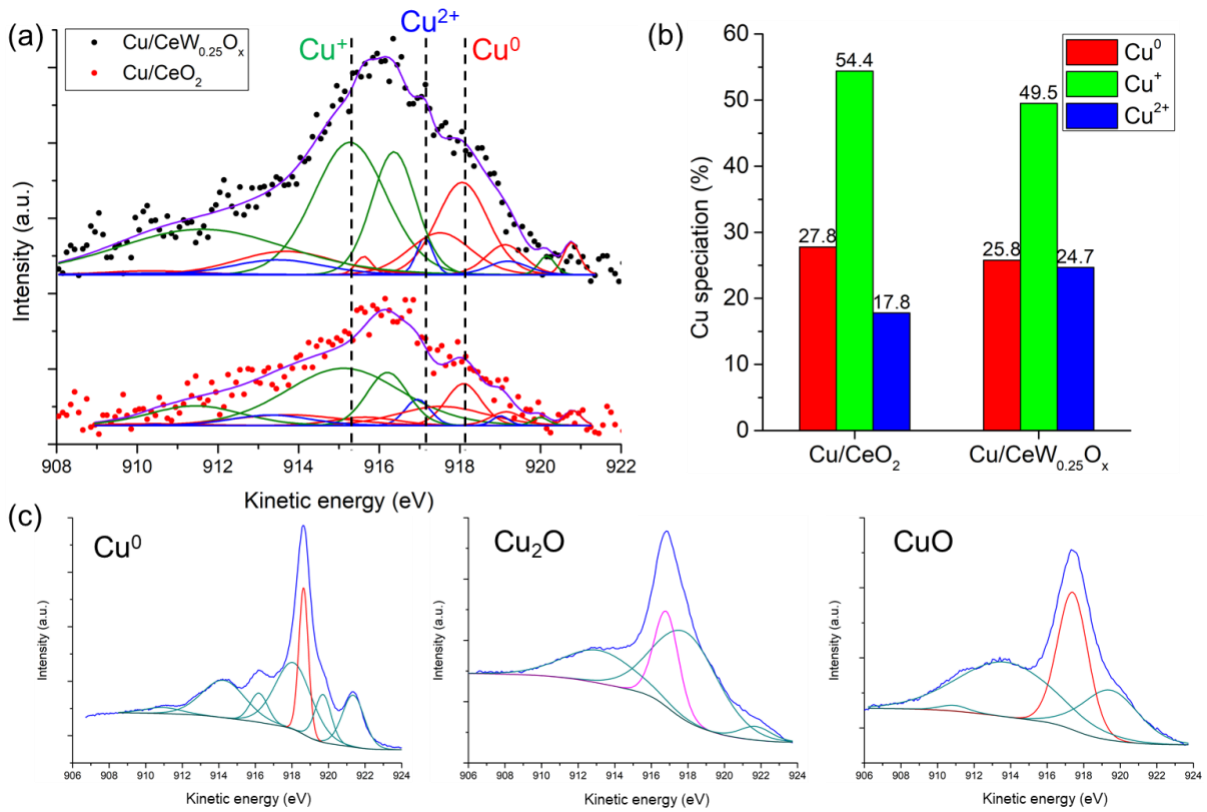

Figure S4. (a) Cu Auger spectra of Cu/CeO_2 and $Cu/CeW_{0.25}O_x$ catalysts; the red, green, blue and purple curves represent the fitted profiles of Cu^0, Cu^+, Cu^{2+} and the sum of all fitted peaks, respectively. (b) Results of quantitative analysis of the Cu Auger spectra. (c) Reference Auger spectra of Cu^0, Cu_2O, and CuO.

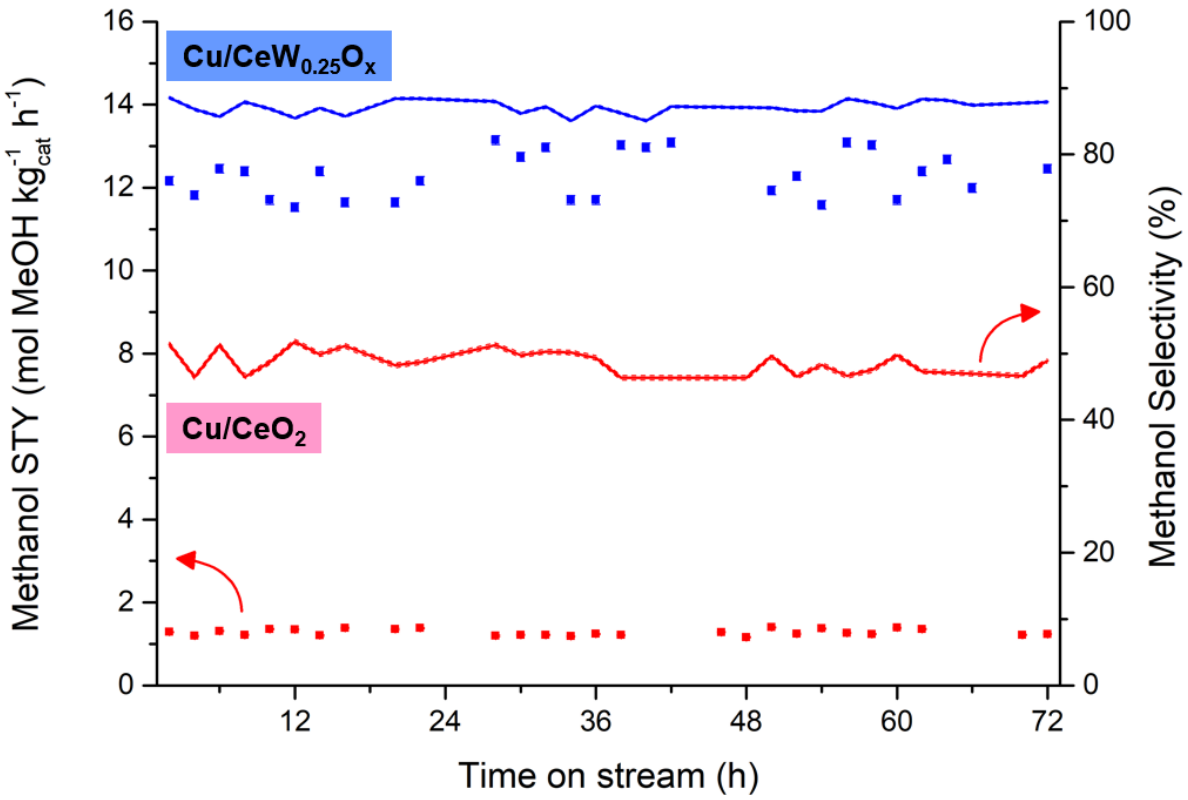

Figure S5. Methanol STY and selectivity over Cu/CeO_2 and $Cu/CeW_{0.25}O_x$ catalysts during CO_2 hydrogenation in a 23:69:8 mixture of $CO_2/H_2/N_2$ at 250 °C, 35 bar, with a WHSV of 15000 mL g_{cat}^{-1} h^{-1}, over 72 h time-on-stream. The dotted lines represent the 1 standard error of the methanol selectivities, estimated based on the variability between the data points.

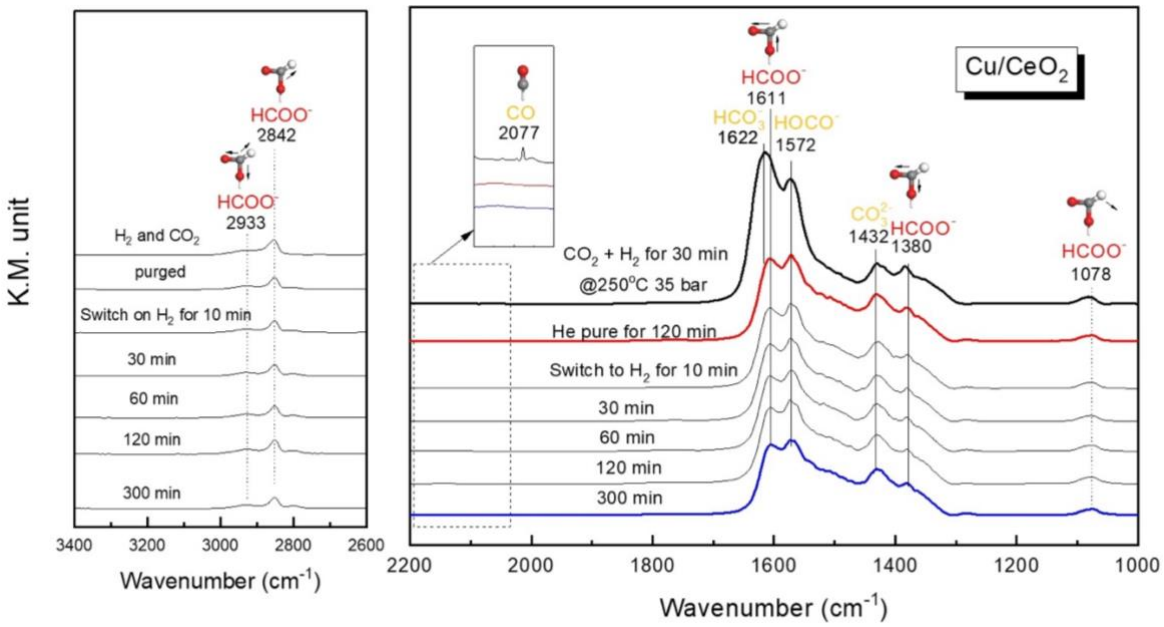

Figure S6. DRIFTS spectra recorded when Cu/CeO_2 was exposed to a 23:69:8 mixture of $CO_2/H_2/N_2$ at 250 °C for 30 min, followed by He purge for 120 min and then switching on H_2 only. All measurements were performed in 35 bar total pressure.

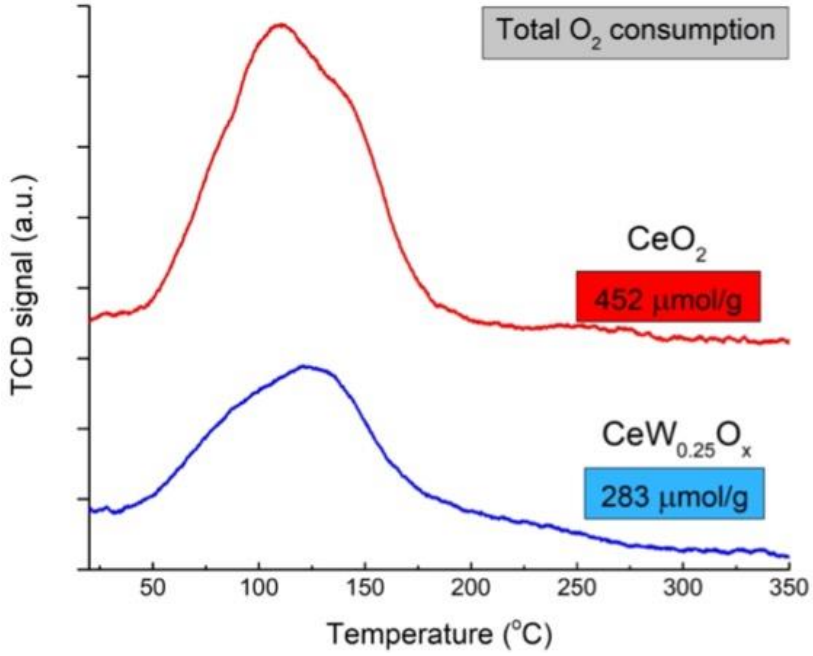

Figure S7. O_2-TPO profiles of the pre-reduced supports.

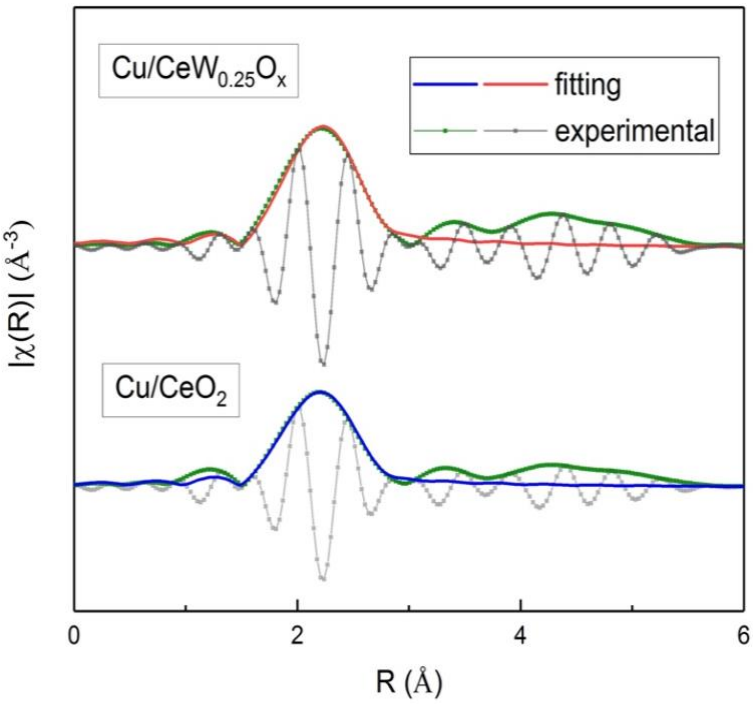

Figure S8. k_3-weighted Fourier transforms of the Cu EXAFS data of the Cu/CeO_2 and $Cu/CeW_{0.25}O_x$ after reduction in 10% H_2/He at 500 °C, 10 bar total pressure.

Table S1. Results of ICP-OES analysis of Cu loading and N_2O chemisorption analysis of Cu dispersion on Cu/CeO_2 and $Cu/CeW_{0.25}O_x$.

Sample	Cu loading	Dispersion
Cu/CeO_2	9.8 wt%	16.8 %
$Cu/CeW_{0.25}O_x$	10.9 wt%	16.9 %

Table S2. Comparison of the methanol synthesis activity of the Cu/CeO_2-based catalysts investigated in the present study and those reported in the literature.

Catalyst	Cu loading (wt.%)	T (°C)	P (MPa)	WHSV (mL g_{cat}^{-1} h^{-1})	H_2:CO_2	Conv. (%)	Sel. (%)	STY		Ref
								$mol_{MeOH} \cdot kg_{cat}^{-1} \cdot h^{-1}$	$kg_{MeOH} \cdot kg_{cat}^{-1} \cdot h^{-1}$	
Cu/CeO_2	9.8	250	3.5	15000	3	1.3	51	1.26	0.0403	This work
$Cu/CeW_{0.25}O_x$	10.9	250	3.5	15000	3	13	87	12.32	0.394	This work
$Cu/CeTiO_x$	25.5	235	3	2000	3	6.5	33	1.11	0.0355	[1]
Cu/CeO_2	4.6	250	3	30000	3	1.6	50	2.1	0.0672	[2]
Cu/CeO_2	8.9	300	5	45000	5	28	10	2.84	0.0909	[3]
Cu/CeO_2	5	240	2	3000	3	2.1	90	0.636	0.0204	[4]
Cu/CeO_2	35	280	3	10000	3	10.1	42	2.12	0.0678	[5]

Table S3. The apparent activation energy of both CO and methanol formation estimated from the Arrhenius-plot. The error estimated represents one standard deviation of the estimated Arrhenius constants.

Sample	$E_{a,CO}$ (kJ/mol)	$E_{a,methanol}$ (kJ/mol)
Cu/CeO_2	54.8 ± 5.0	58.2 ± 2.1
$Cu/CeW_{0.25}O_x$	52.7 ± 2.5	38.0 ± 1.9

Table S4. The active oxygen vacancies obtained from CO_2-TPD profiles and the O_2 consumption by O_2-TPO.

Sample	CeO_2	$CeW_{0.25}O_x$	Cu/CeO_2	$Cu/CeW_{0.25}O_x$
Active vacancy volume (μmol/g)	144	103	121	78
O_2 consumption (μmol/g)	452	283	-	-

Table S5. The mole fraction of Ce^{3+} in the catalysts at the various stages of in situ XANES experiment, estimated by the linear combination fitting analysis of the Ce L_{III} edge spectra.

Catalyst	Cu/CeO_2	$Ce/CeW_{0.25}O_x$
Freshly calcined in air	0	49%
Reduced by H_2	17%	69%
During CO_2 hydrogenation	15%	59%

Table S6. The fitting parameters of Cu EXAFS.

Sample	Cu-Cu Coordination Number	R(Å)	δ^2	ΔE_0
Cu/CeO_2	9.1	2.531	0.0129	4.059
$Cu/CeW_{0.25}O_x$	9.5	2.539	0.0058	5.429

References

[1] K. Chang, T. Wang, J.G. Chen, Hydrogenation of CO2 to methanol over CuCeTiOx catalysts, Applied Catalysis B: Environmental. 206 (2017) 704–711. https://doi.org/10.1016/j.apcatb.2017.01.076.

[2] J. Zhu, Y. Su, J. Chai, V. Muravev, N. Kosinov, E.J.M. Hensen, Mechanism and Nature of Active Sites for Methanol Synthesis from CO/CO2 on Cu/CeO2, ACS Catal. 10 (2020) 11532–11544. https://doi.org/10.1021/acscatal.0c02909.

[3] P. Sripada, J. Kimpton, A. Barlow, T. Williams, S. Kandasamy, S. Bhattacharya, Investigating the dynamic structural changes on Cu/CeO2 catalysts observed during CO2 hydrogenation, Journal of Catalysis. 381 (2020) 415–426. https://doi.org/10.1016/j.jcat.2019.11.017.

[4] B. Ouyang, W. Tan, B. Liu, Morphology effect of nanostructure ceria on the Cu/CeO2 catalysts for synthesis of methanol from CO2 hydrogenation, Catalysis Communications. 95 (2017) 36–39. https://doi.org/10.1016/j.catcom.2017.03.005.

[5] W. Wang, Z. Qu, L. Song, Q. Fu, CO2 hydrogenation to methanol over Cu/CeO2 and Cu/ZrO2 catalysts: Tuning methanol selectivity via metal-support interaction, Journal of Energy Chemistry. 40 (2020) 22–30. https://doi.org/10.1016/j.jechem.2019.03.001.